The cisplatin-based Pt(IV)-diclorofibrato multi-action anticancer prodrug exhibits excellent performances also in hypoxic conditions

Elisabetta Gabano,[a*] Mauro Ravera,[a] Francesca Trivero,[a] Stefano Tinello,[a] Andrea Gallina,[a] Ilaria Zanellato,[a] Marzia B. Gariboldi,[b] Elena Monti,[b] Domenico Osella,[a]

[a] Dipartimento di Scienze e Innovazione Tecnologica, Università del Piemonte Orientale, Viale Michel 11, 15121 Alessandria, Italy. E-mail: elisabetta.gabano@uniupo.it

[b] Dipartimento di Biotecnologie e Scienze della Vita, Università dell'Insubria, Via Manara 7, 21052 Busto Arsizio (VA).

ELECTRONIC SUPPORTING INFORMATION

Content:

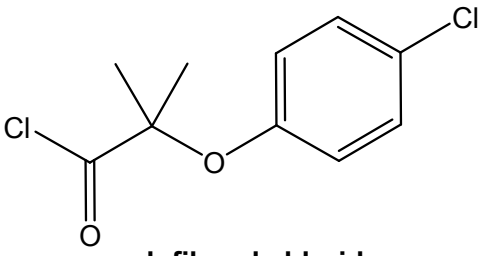

clofibroyl chloride

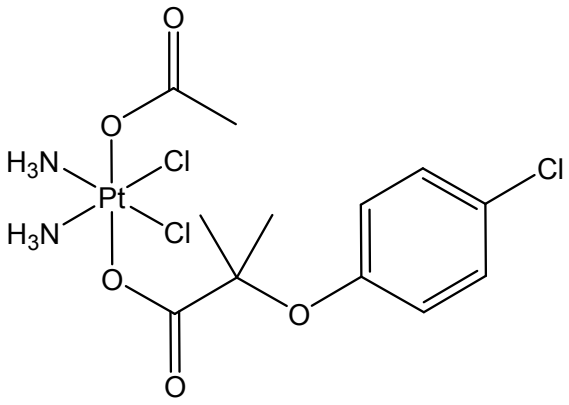

1

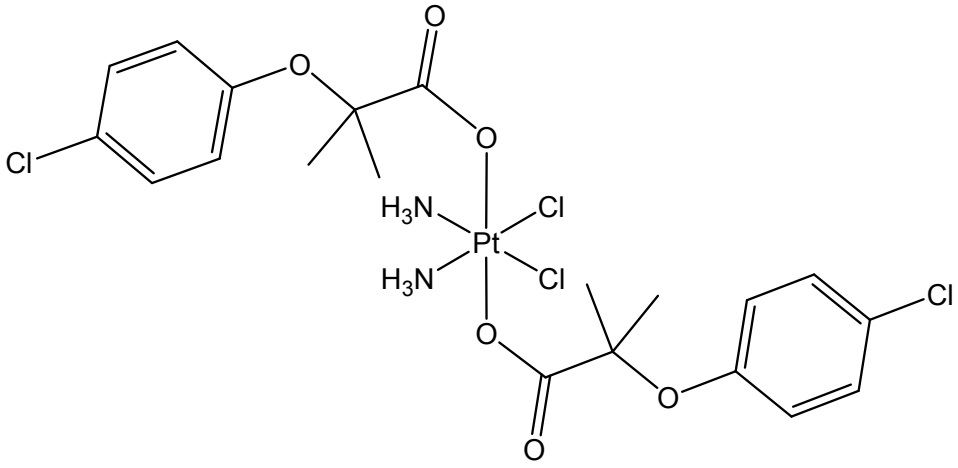

2

Figure S0. Sketch of the complexes under investigation

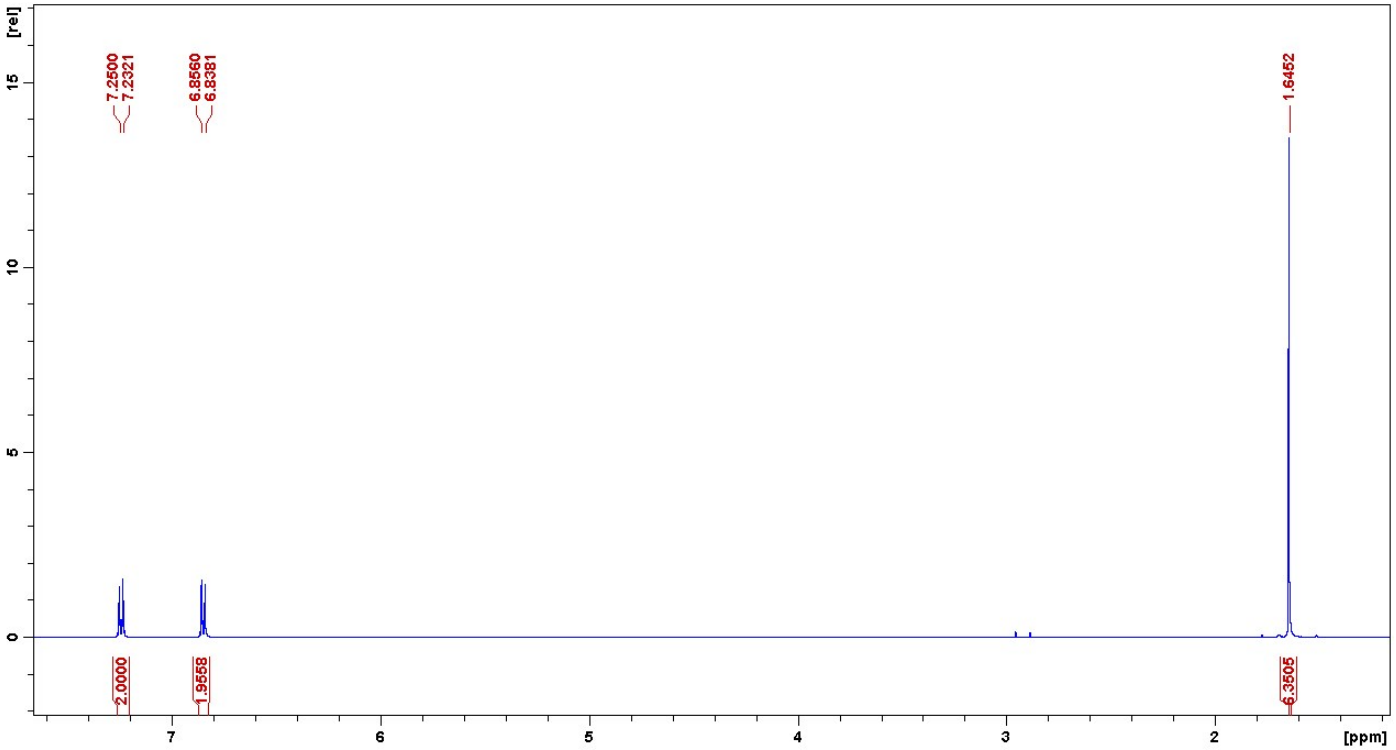

Figure S1. ^{1}H NMR spectrum of clofibroyl chloride in $CDCl_3$

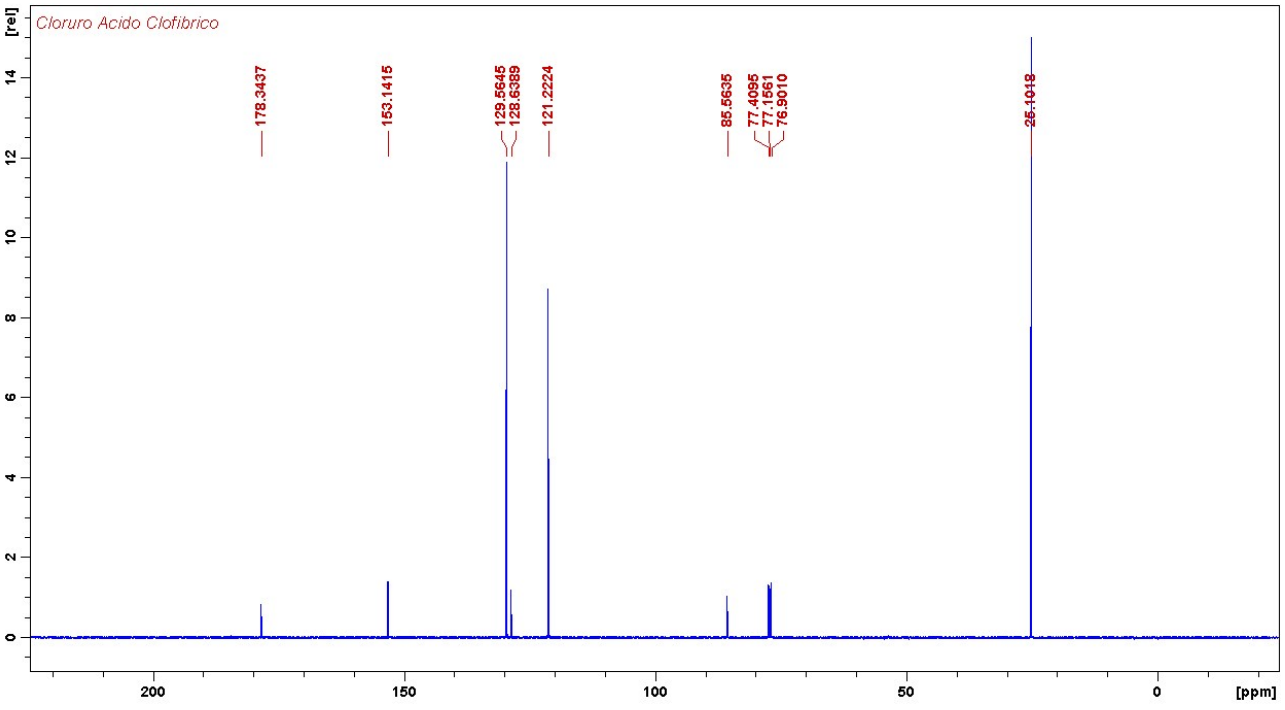

Figure S2. $^{13}C\{^{1}H\}$ NMR spectrum of clofibroyl chloride in $CDCl_3$

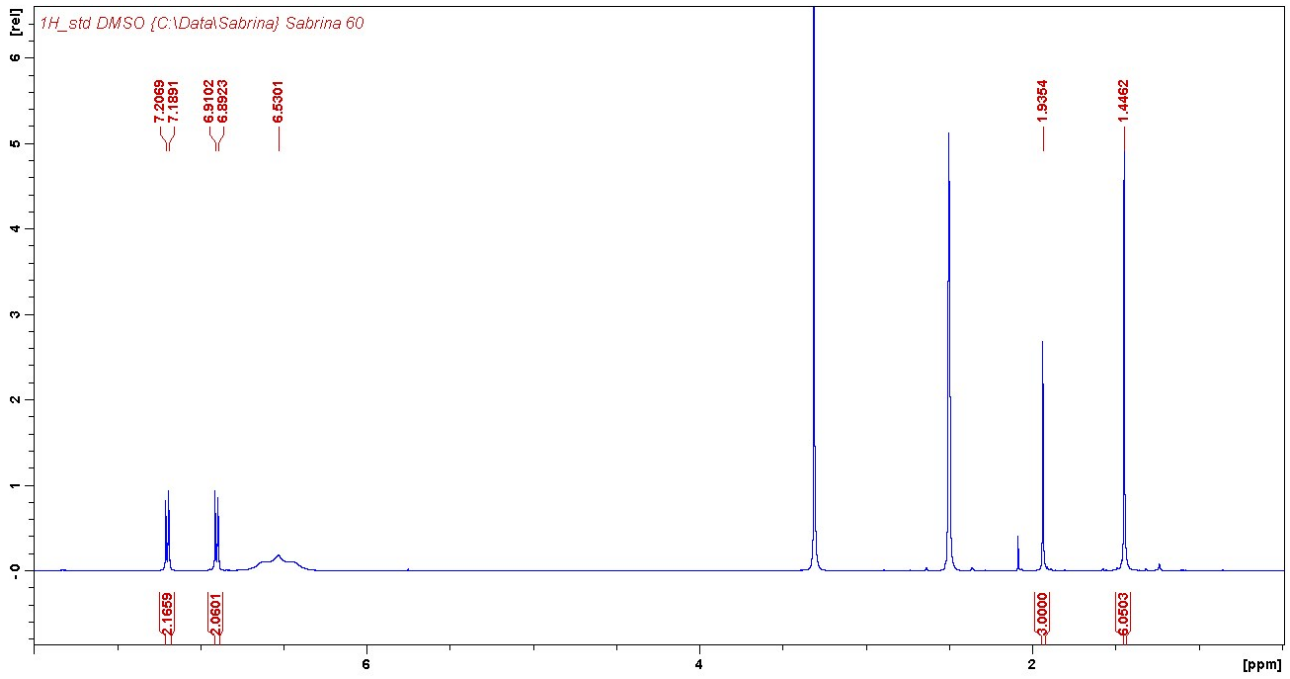

Figure S3: ^{1}H NMR spectrum of complex **1** in DMSO-d_6 (residual acetone is observed at ca. 2.1 ppm).

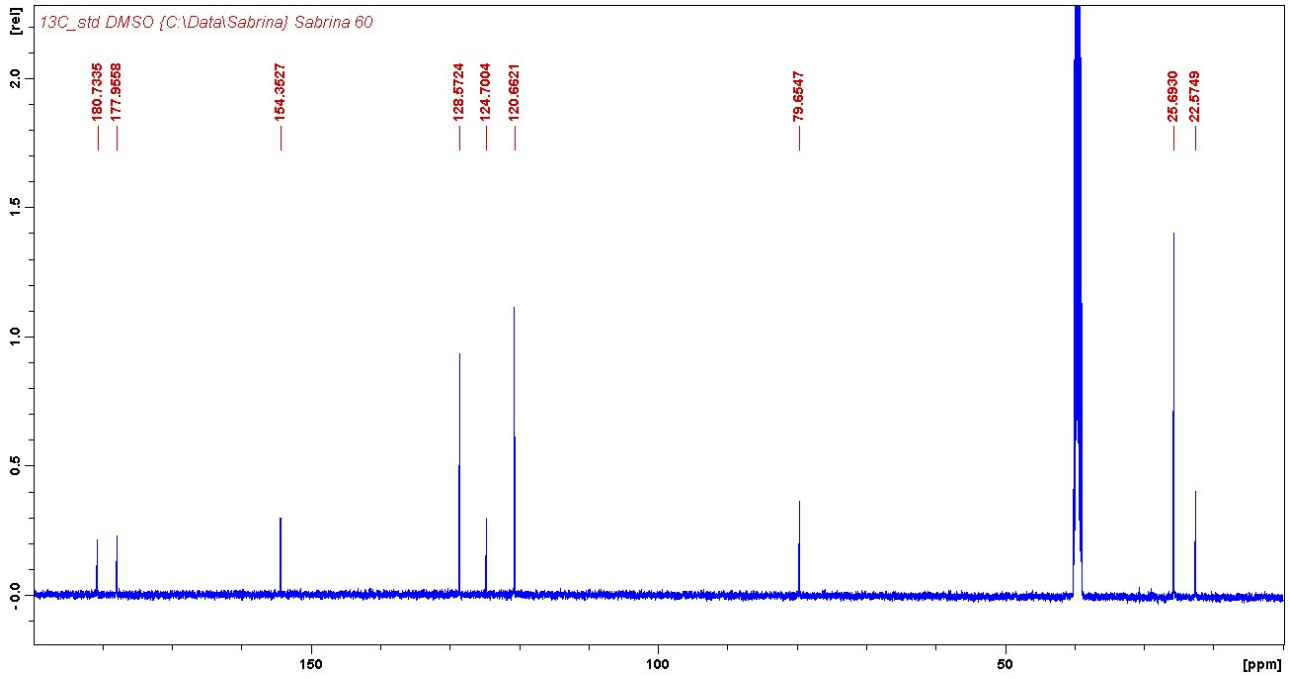

Figure S4: $^{13}C\{^{1}H\}$ NMR spectrum of complex **1** in DMSO-d_6.

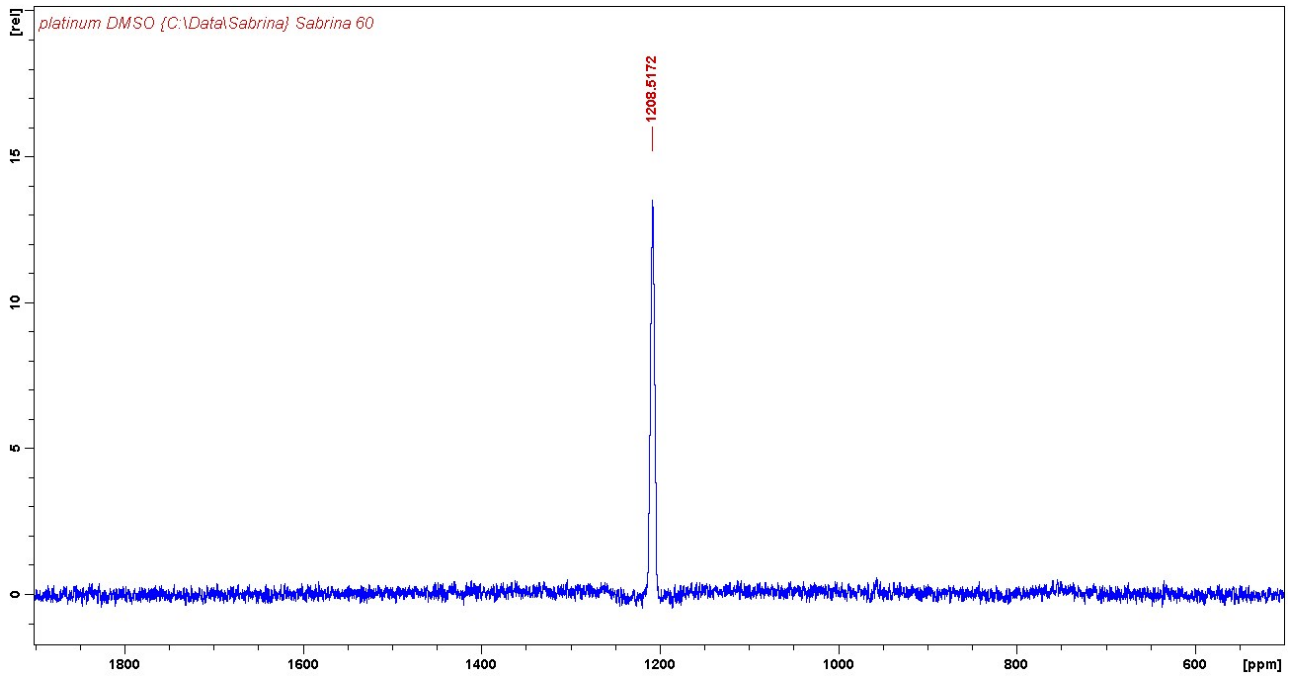

Figure S5: ^{195}Pt NMR spectrum of complex **1** in DMSO-d_6.

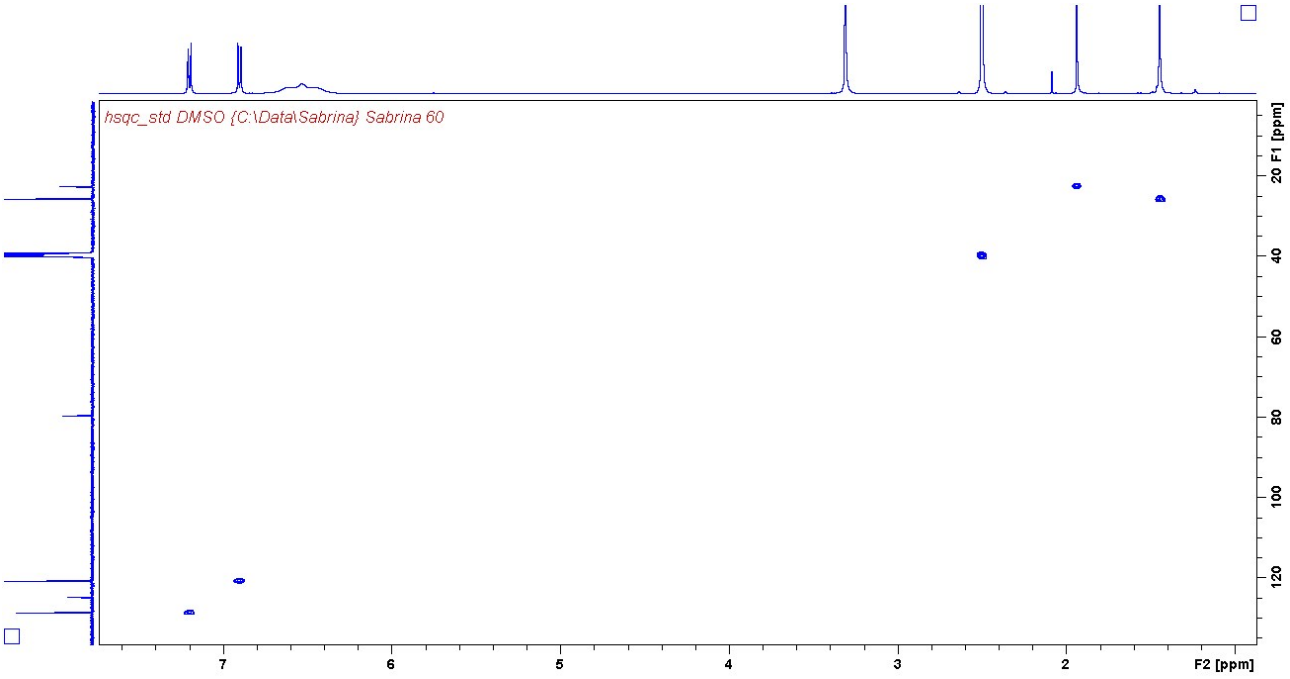

Figure S6: [^{1}H, ^{13}C] HSQC NMR spectrum of complex **1** in DMSO-d_6.

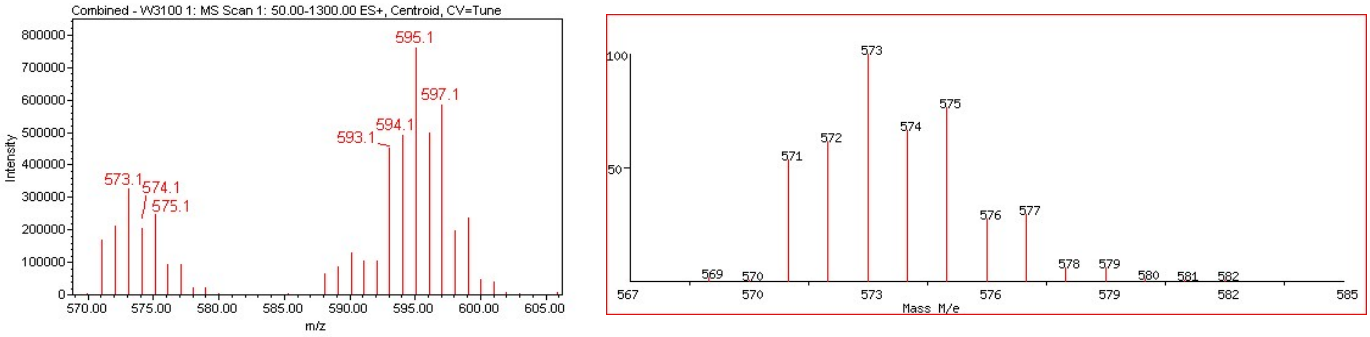

Figure S7: ESI-MS NMR spectrum of complex **1** showing both the $[M+H]^+$ and $[M+Na]^+$ species and simulation for the $[M+H]^+$ species

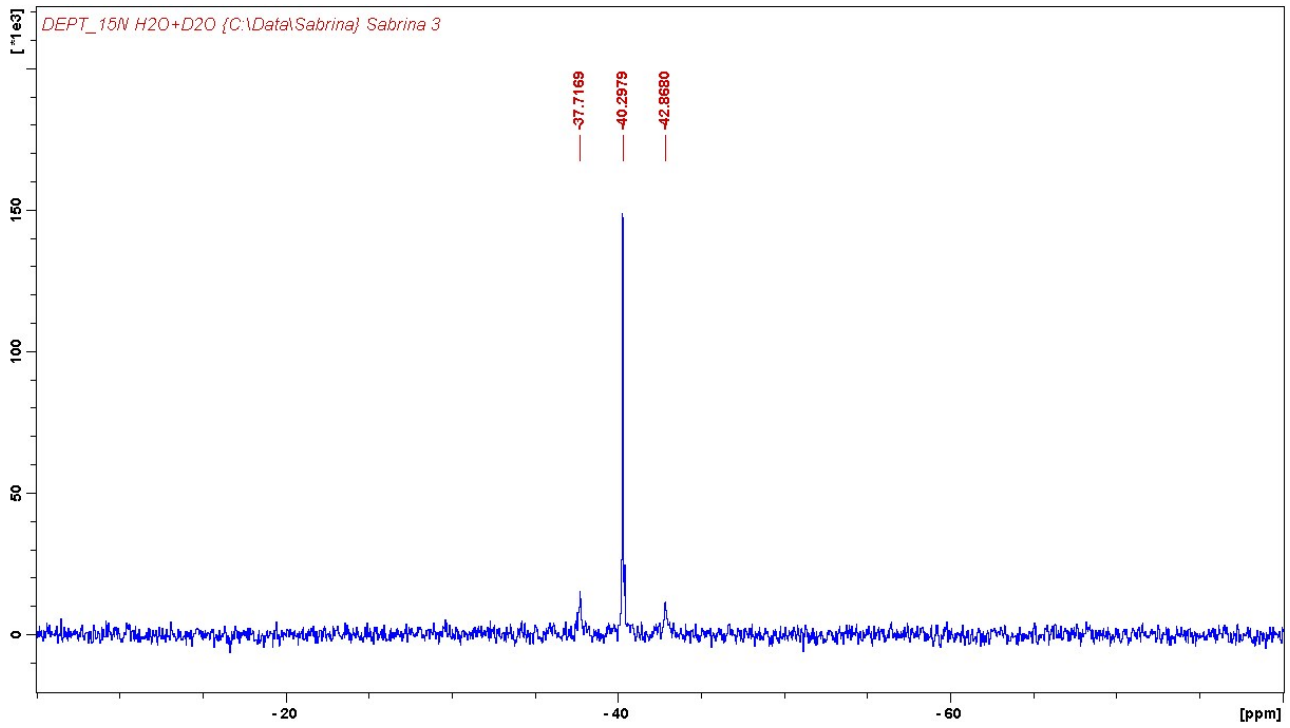

Figure S8: $^{15}N\{^{1}H\}$ DEPT-45 NMR spectrum of **^{15}N-1**

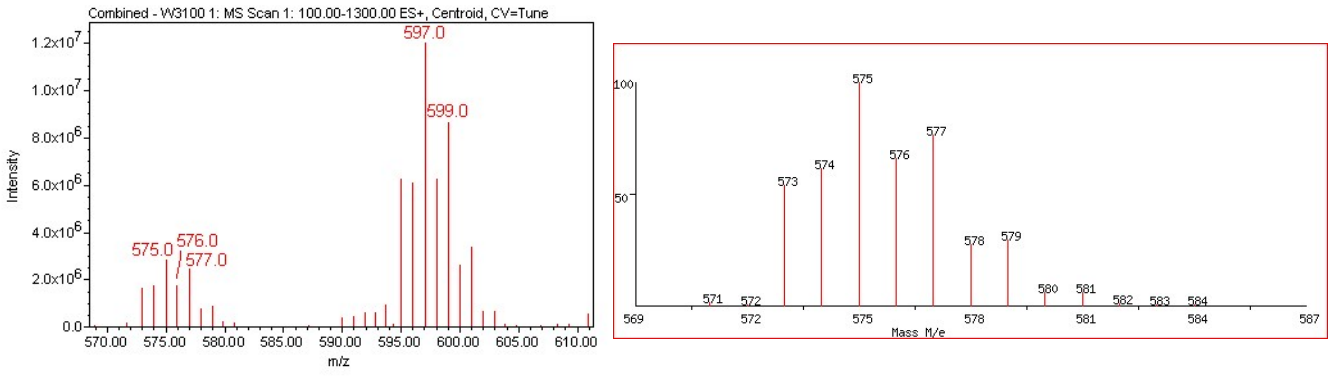

Figure S9: ESI-MS NMR spectrum of complex **^{15}N-1** showing both the $[M+H]^+$ and $[M+Na]^+$ species and simulation for the $[M+H]^+$ species

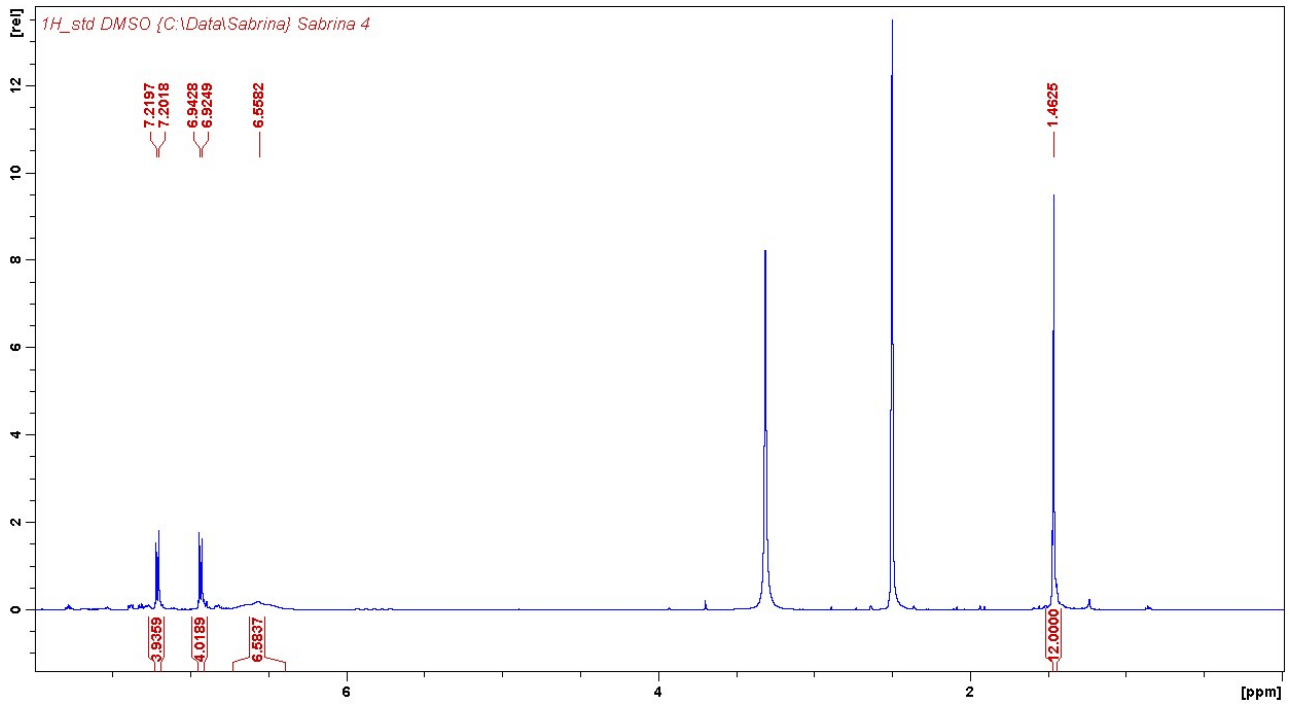

Figure S10: ^{1}H NMR spectrum of complex **2** in DMSO-d_6.

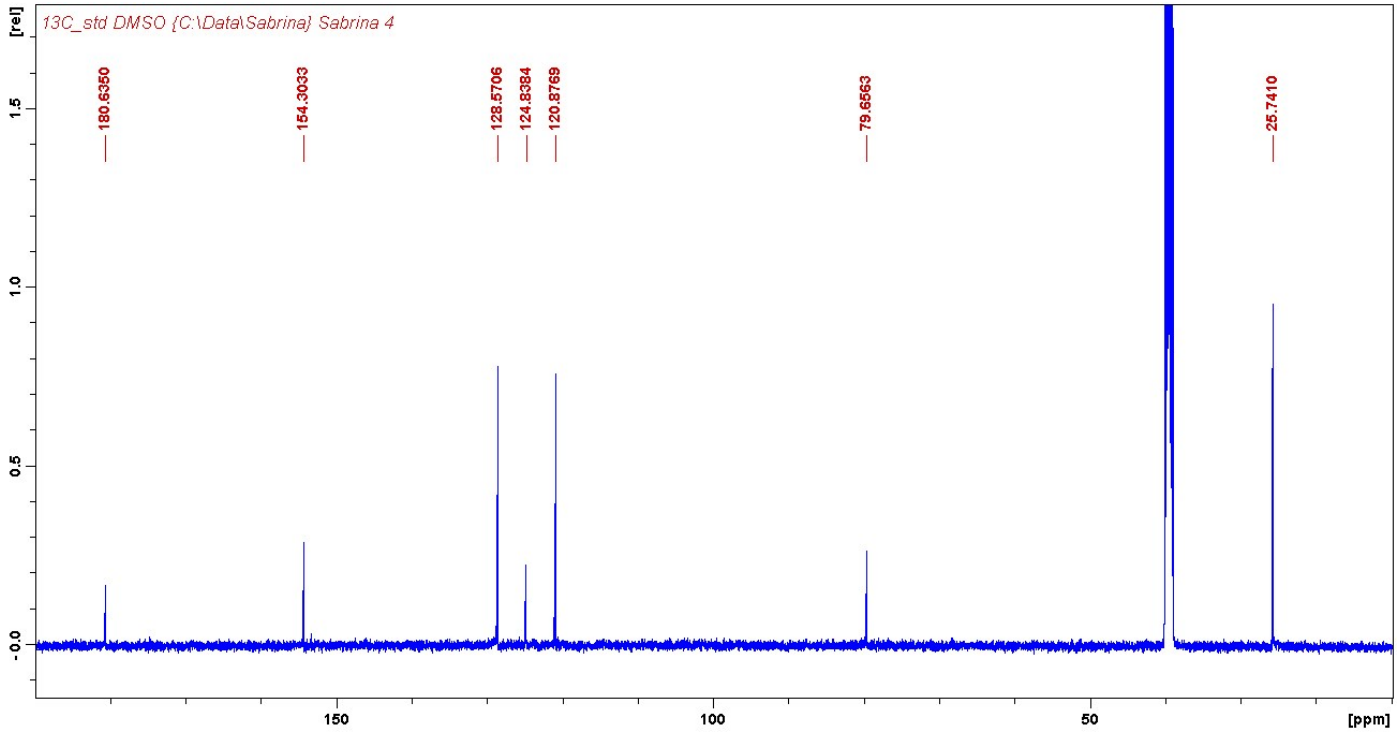

Figure S11: ^{13}C{^{1}H} NMR spectrum of complex **2** in DMSO-d_6.

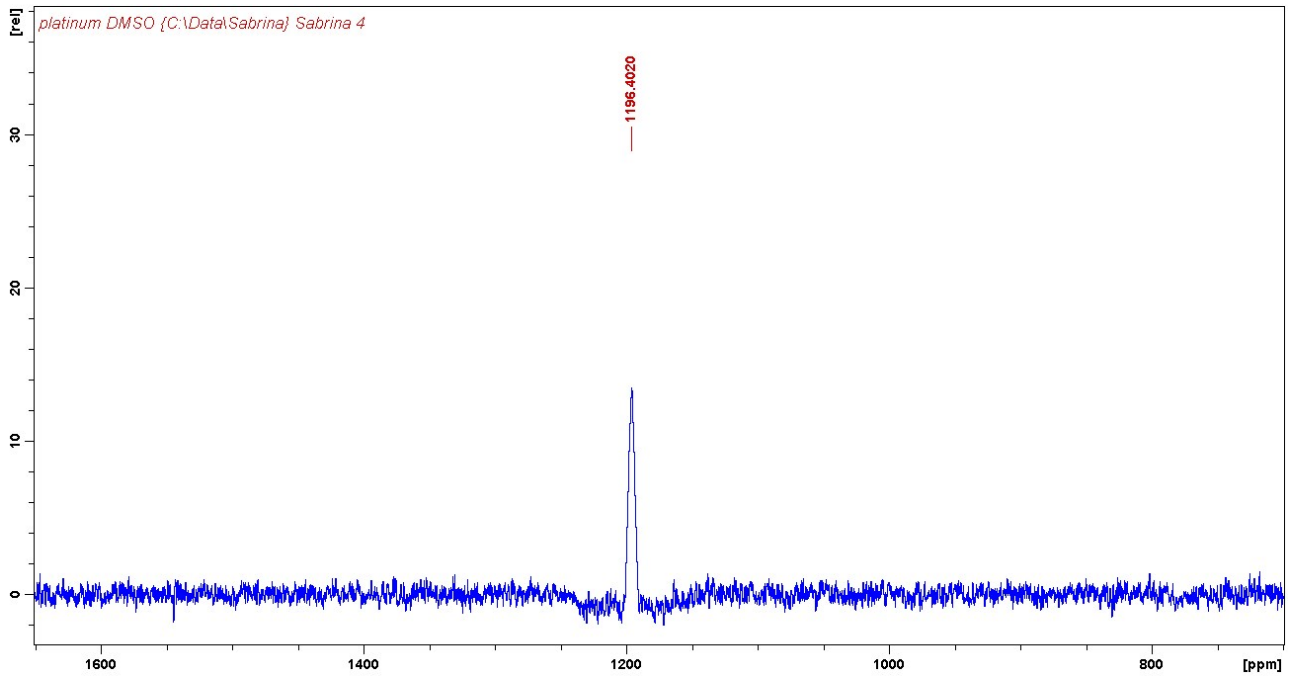

Figure S12: ^{195}Pt NMR spectrum of complex **2** in DMSO-d_6.

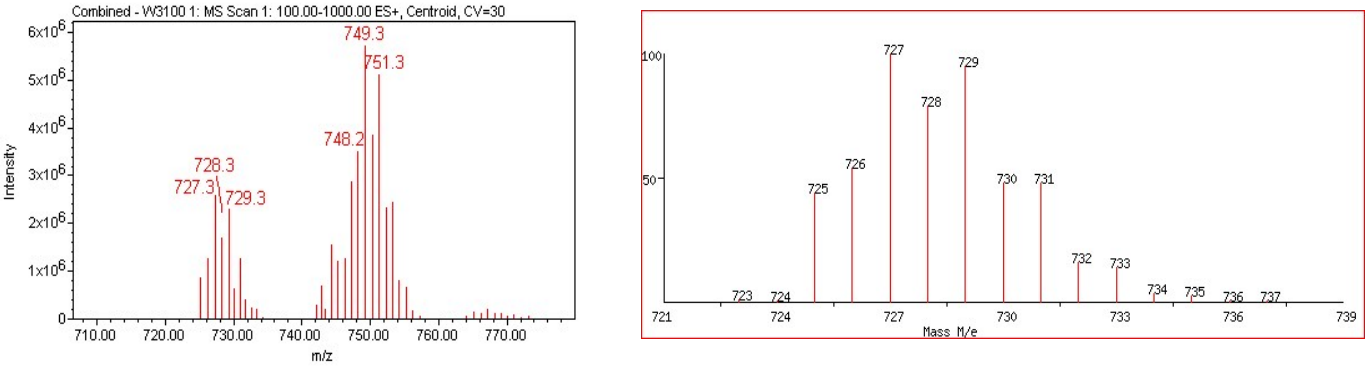

Figure S13: ESI-MS NMR spectrum of complex **2** showing both the $[M+H]^+$ and $[M+Na]^+$ species and simulation for the $[M+H]^+$ species

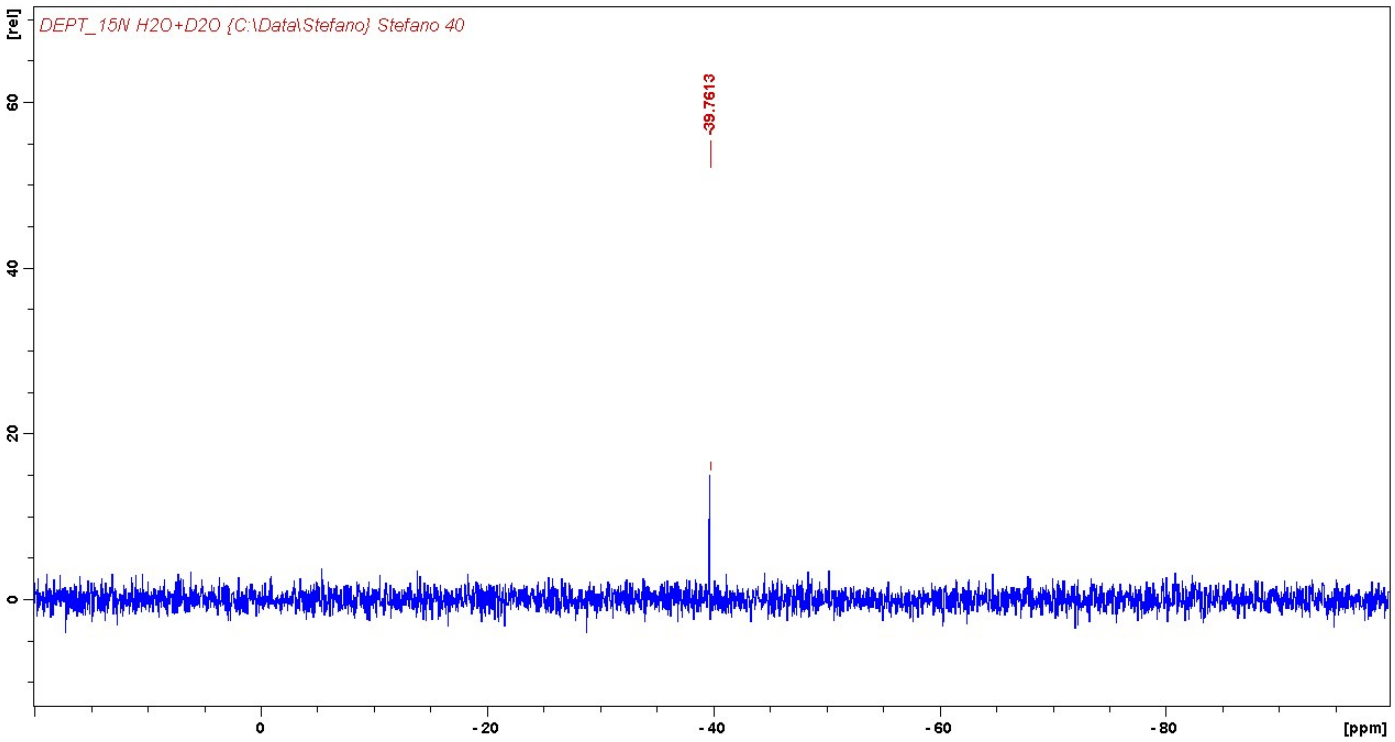

Figure S14: $^{15}N\{^{1}H\}$ DEPT-45 NMR spectrum of complex **^{15}N-2**

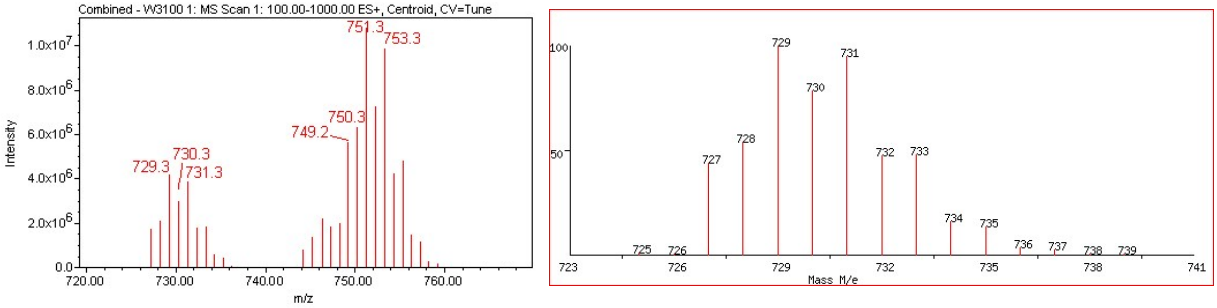

Figure S15: ESI-MS NMR spectrum of complex **^{15}N-2** showing both the $[M+H]^+$ and $[M+Na]^+$ species and simulation for the $[M+H]^+$ species

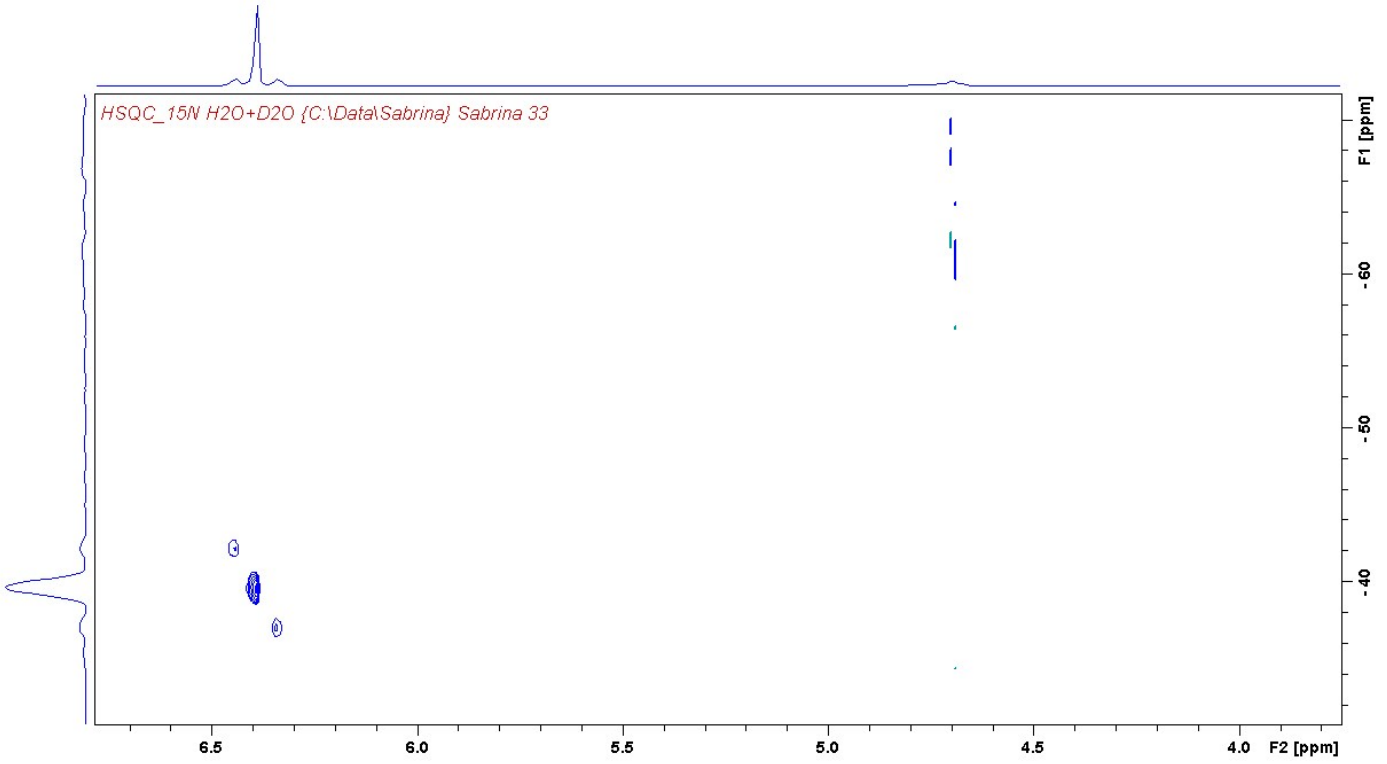

Figure S16: [^{1}H, ^{15}N] HSQC spectrum of complex **^{15}N-1**

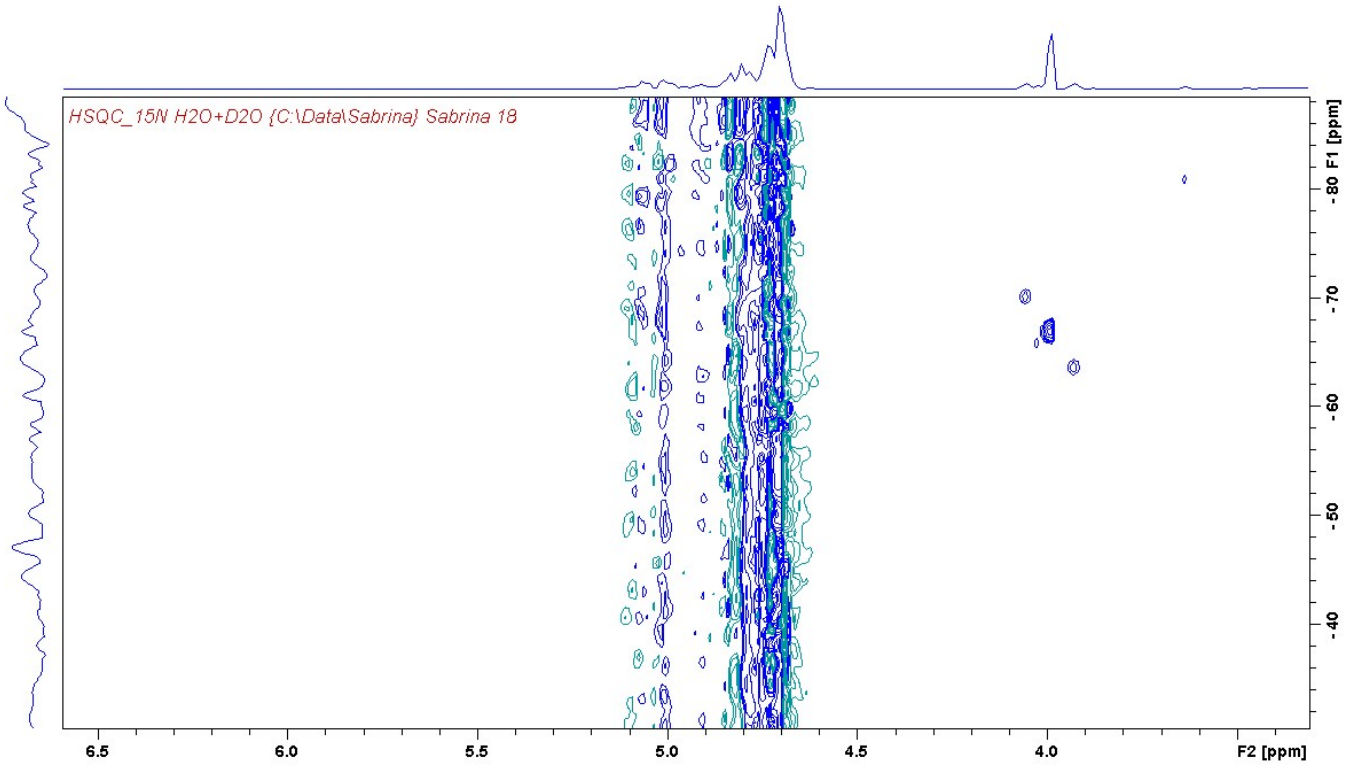

Figure S17: [^{1}H, ^{15}N] HSQC spectrum for the reduction of complex **^{15}N-1** with cell extracts

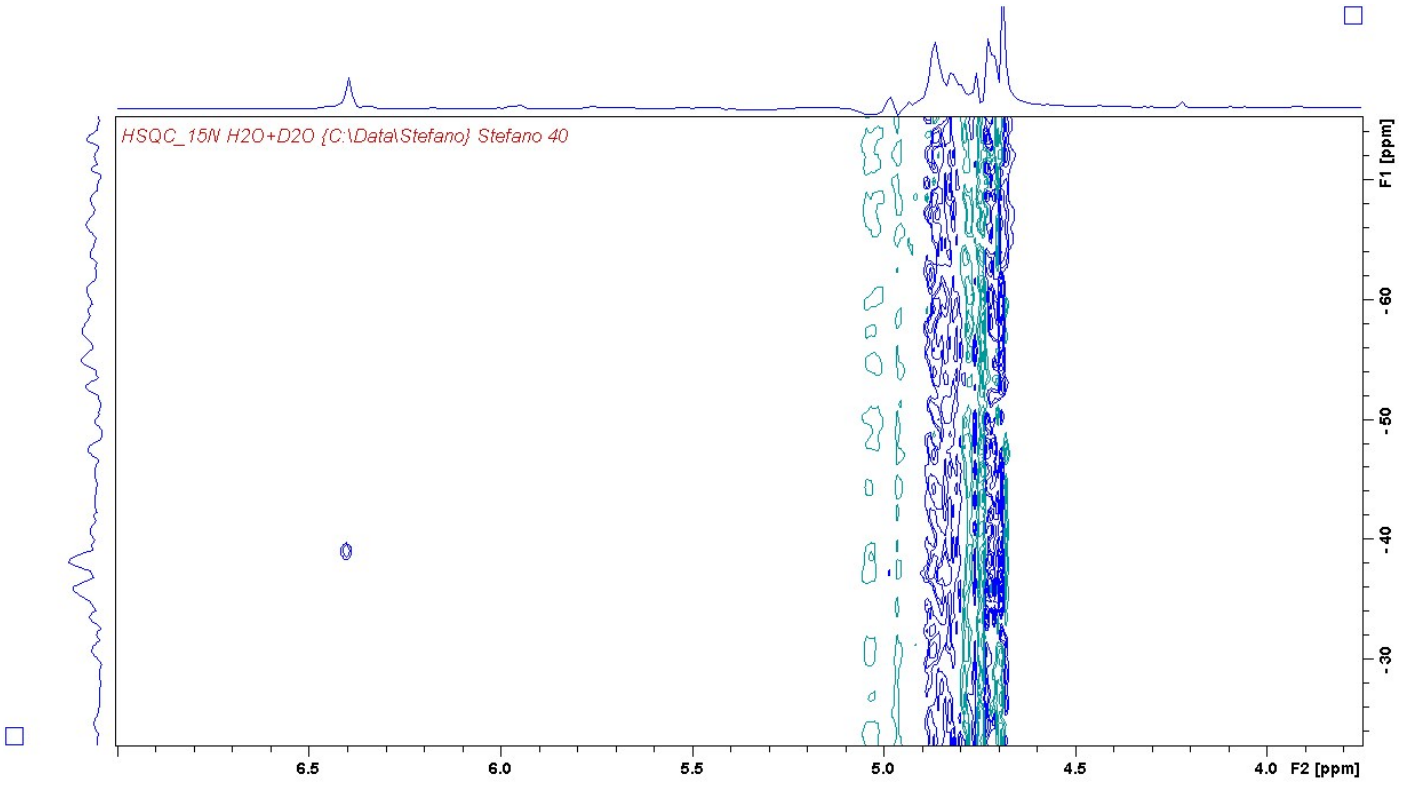

Figure S18: [^{1}H, ^{15}N] HSQC spectrum of complex **^{15}N-2**

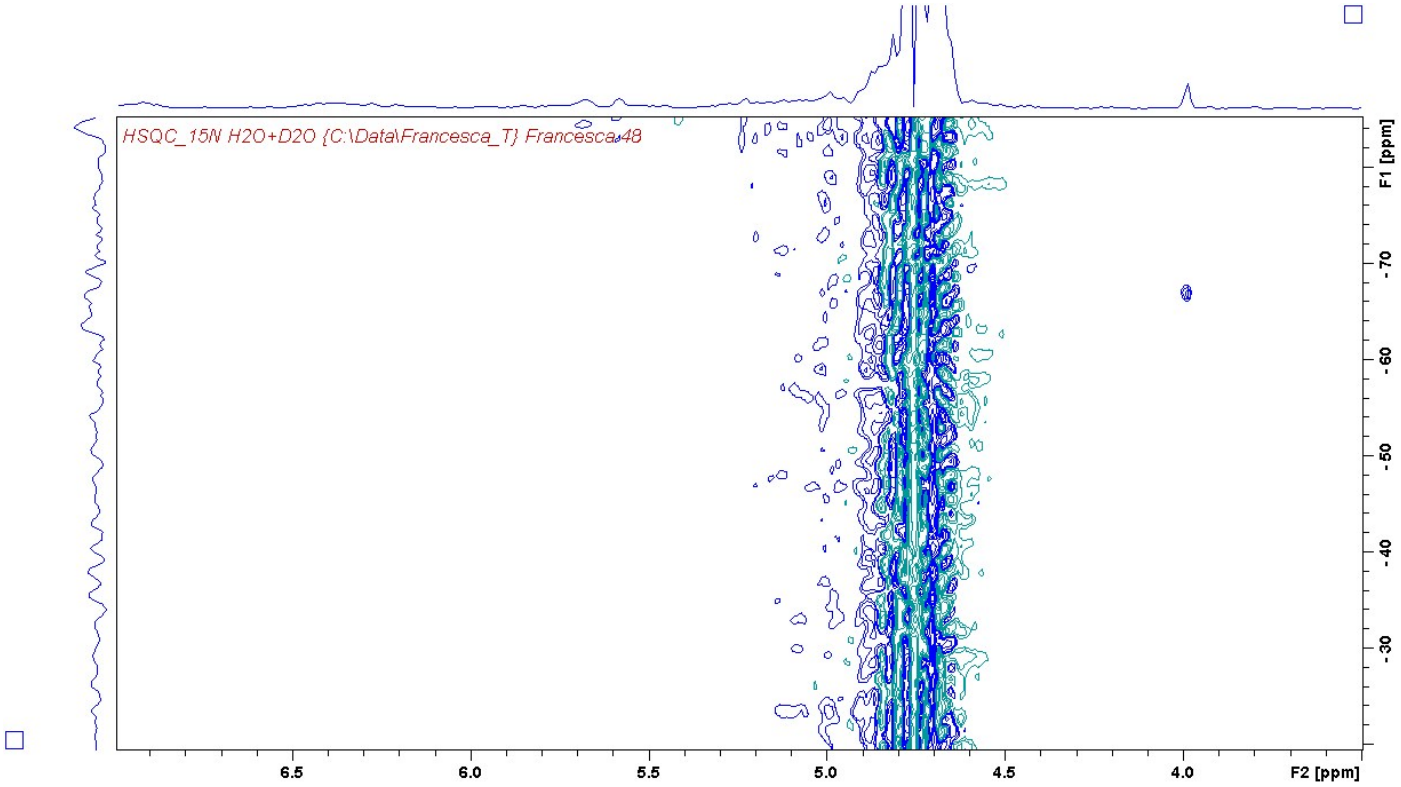

Figure S19: [^{1}H, ^{15}N] HSQC spectrum for the reduction of complex **^{15}N-2** with cell extracts

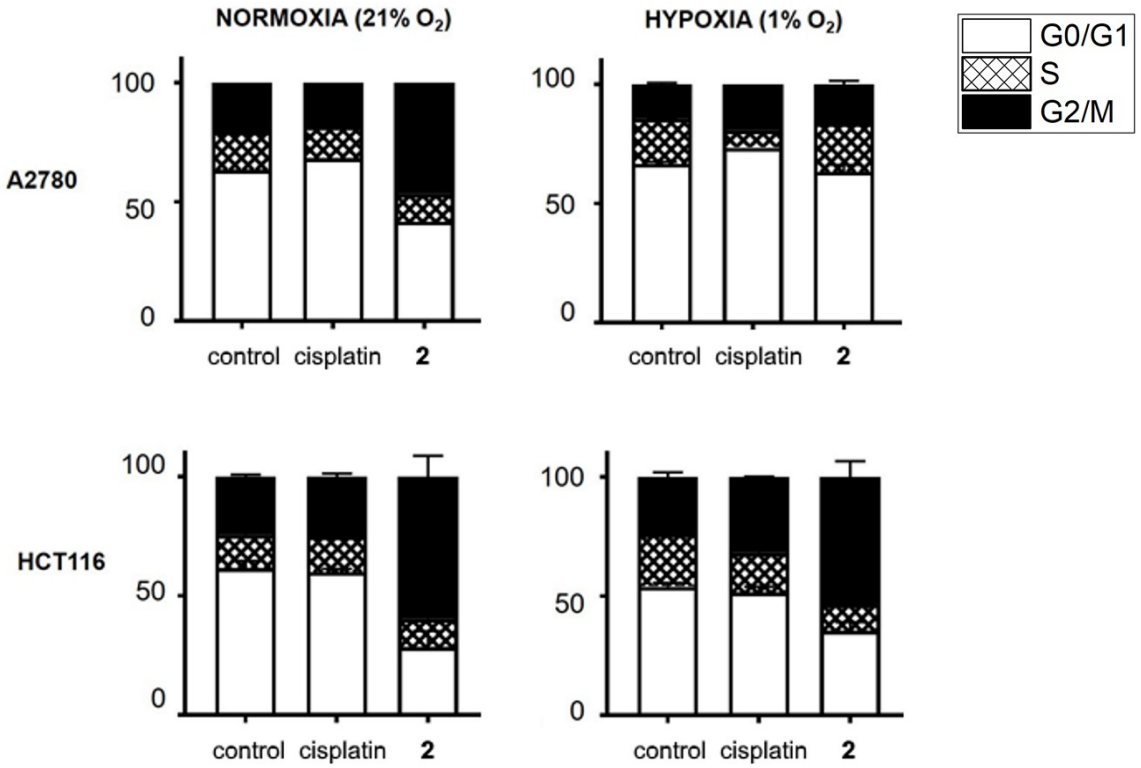

Figure S20: Cell cycle distribution of A2780 cells (top plots) and HCT 116 (bottom plots) after 48 h CT with equitoxic concentrations of cisplatin and **2** in normoxic (left plots) and hypoxic conditions (right plots). The *abscissa* of each plot represents the percentage of cells among the cell cycle phases. Data are means ± standard error means of at least three independent samples.

Table S1. Genes analyzed by means of Quantitative Reverse Transcription PCR (RT-qPCR). The NCBI accession number is reported along with the 5'-3' sequence of the forward and reverse primer and the expected product length.

Gene	Accession n°	Forward	Reverse	Product lenght (bp)
ACOX1	NM_004035.6	GCTGGAGCTGCGGATTTAGA	TGTTCTCGATCTCTCGGCGG	187
ACOX1	NM_001876.3	CACTGAGCACGGCAAGATGAG	AGGCGAGGCAGCGATGTC	111
Cyclin D1 (CCND1)	NM_053056.2	TGAGGGACGCTTTGTCTGTC	GCCTTTGGCCTCTCGATACA	75
p21 (CDKN1A)	NG_009364	GCGACTGTGATGCGCTAATG	GAAGGTAGAGCTTGGGCAGG	141
Cyclin A2 (CCNA2)	NM_001237.4	TGGTGGTCTGTGTTCTGTGA	TGCCAGTCTTACTCATAGCTGA	136
Cyclin E (CCNE)	NM_001238	GCAGGATCCAGATGAAGAAATG	TAATCCGAGGCTTGCACGTT	173
HMOX1	NM_002133.2	TCTTGGCTGGCTTCCTTACC	GGATGTGCTTTTCGTTGGGG	123
TP53 (p53)	NG_017013.2	GCCCCTCCTCAGCATCTTATC	CTCATAGGGCACCACCACAC	99
GAPDH	NG_007073.2	ATCCCTGAGCTGAACGGGAA	GGCAGGTTTTTCTAGACGGC	99
HPRT1	NM_000194.2	TTGCTTTCCTTGGTCAGGCA	ATCCAACACTTCGTGGGGTC	85
RNA18SN1	NR_145820.1	CGTCTGCCCTATCAACTTTCG	TGCCTTCCTTGGATGTGGTAG	124